Amyloid-β Peptides

International Edition: DOI: 10.1002/anie.201604970
German Edition: DOI: 10.1002/ange.201604970

Nucleation of Amyloid Oligomers by RepA-WH1-Prionoid-Functionalized Gold Nanorods

Cristina Fernández[+], Guillermo González-Rubio[+], Judith Langer, Gloria Tardajos, Luis M. Liz-Marzán, Rafael Giraldo, and Andrés Guerrero-Martínez**

Abstract: *Understanding protein amyloidogenesis is an important topic in protein science, fueled by the role of amyloid aggregates, especially oligomers, in the etiology of a number of devastating human degenerative diseases. However, the mechanisms that determine the formation of amyloid oligomers remain elusive due to the high complexity of the amyloidogenesis process. For instance, gold nanoparticles promote or inhibit amyloid fibrillation. We have functionalized gold nanorods with a metal-chelating group to selectively immobilize soluble RepA-WH1, a model synthetic bacterial prionoid, using a hexa-histidine tag (H6). H6-RepA-WH1 undergoes stable amyloid oligomerization in the presence of catalytic concentrations of anisotropic nanoparticles. Then, in a physically separated event, such oligomers promote the growth of amyloid fibers of untagged RepA-WH1. SERS spectral changes of H6-RepA-WH1 on spherical citrate-AuNP substrates provide evidence for structural modifications in the protein, which are compatible with a gradual increase in β-sheet structure, as expected in amyloid oligomerization.*

Protein amyloidoses such as Alzheimer's, Parkinson's, and prion-related diseases are the focus of intense research due to their deep impact on human health.[1] Amyloidogenesis is a nearly universal process for the conformational conversion between the native and aggregated states of proteins, with implications for essential physiological processes.[2] Among the distinct association states that any protein transits from the native and soluble states to the fully aggregated amyloid condition, that is, small oligomeric assemblies, large oligomers, and fibers, the first are the most toxic and thus disease-relevant species.[3]

Among the experimental techniques used to characterize amyloidogenesis in vitro, spectroscopy occupies a central position. Namely, UV/Vis absorption spectroscopy has been used to study the binding of the amyloidotropic stain Congo red, often detected as green birefringence under a polarized light microscope.[4] Fluorescence spectroscopy is also used to investigate amyloidogenesis through the binding of extrinsic fluorophores, which increase and/or shift their fluorescence emission upon intercalation between the β-sheets that constitute the characteristic amyloid cross-β fold.[5] For these techniques, a rather mature fibrillar or prefibrillar form is required to achieve sufficient binding of the probes. These molecules are thus not efficient for the investigation of early amyloidogenic oligomers.[1–3]

Surface-enhanced Raman scattering (SERS) spectroscopy has emerged as a useful technique for sensing amyloid proteins at the surface of plasmonic gold nanoparticles (AuNPs),[6] since the chemical nature and 3D arrangement of the proteins determine a unique and enhanced Raman vibrational fingerprint.[7] Analogously to other organic and inorganic nanomaterials,[8] AuNPs features, such as the size, charge, and shape, can either promote[9] or inhibit[10] the templating ability of amyloids due to metal–protein interactions. Although these investigations focused mainly on the formation of fibrillar and prefibrillar amyloids,[11] the direct observation of AuNP-induced nucleation of amyloid oligomers at the early stages of amyloidogenesis by SERS has not been reported.

The synthetic prionoid RepA-WH1, the *N*-terminal domain of the bacterial plasmid replication protein RepA,[5b] is an attractive model system to explore the nucleation of amyloid oligomers. Similarly to the mammalian prion PrP,[12] and besides the protein-to-protein templating of the amyloid conformation, nucleic acids (dsDNA) and acidic phospholipids promote the amyloidosis of RepA-WH1, both in vitro and in vivo.[13] This protein undergoes a substantial conformational change from soluble stable dimers to metastable aggregation-prone monomers that then assemble into amyloid fibers.[14] RepA-WH1, in particular its hyper-amyloidogenic mutant variant A31V, H6-RepA-WH1(A31V), causes in bacteria a type of amyloidosis that shares many features with mammalian neurodegenerative diseases,[15] while remaining bio-safe for humans.

Herein, we describe the formation of amyloid oligomers with different molecular weights, induced by gold nanorods

[*] Dr. C. Fernández,[+] Prof. R. Giraldo
Department of Cellular and Molecular Biology
Centro de Investigaciones Biológicas—CSIC
28040 Madrid (Spain)
E-mail: rgiraldo@cib.csic.es
G. González-Rubio,[+] Prof. G. Tardajos, Dr. A. Guerrero-Martínez
Departamento de Química Física I
Universidad Complutense de Madrid
Avda. Complutense s/n, 28040 Madrid (Spain)
E-mail: aguerrero@quim.ucm.es
G. González-Rubio,[+] Dr. J. Langer, Prof. L. M. Liz-Marzán
BioNanoPlasmonics Laboratory, CIC biomaGUNE
Donostia—20009 San Sebastián (Spain)
Prof. L. M. Liz-Marzán
Ikerbasque, Basque Foundation for Science
48013 Bilbao (Spain)
and
Biomedical Research Networking Center in Bioengineering, Biomaterials, and Nanomedicine, CIBER-BBN (Spain)
[+] These authors contributed equally to this work.

Supporting information for this article can be found under: http://dx.doi.org/10.1002/anie.201604970.

(AuNRs) functionalized with the H6-RepA-WH1(A31V) prionoid. Furthermore, we used such oligomers to trigger the growth of amyloid fibril superstructures (Scheme 1). AuNRs were chosen over the more commonly-used spherical AuNPs due to their higher sensitivity to small changes in their dielectric environments, combined with a high reactivity, which facilitates molecular functionalization.[16]

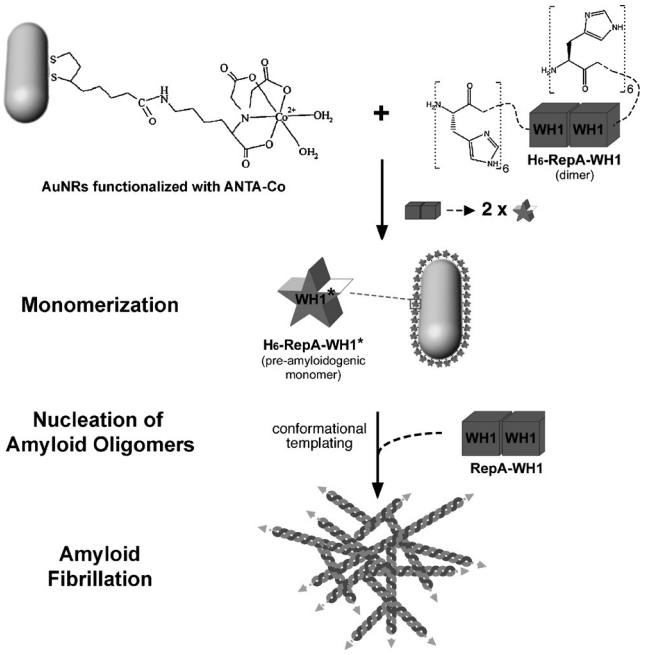

Scheme 1. Outline of the nucleation of RepA-WH1 amyloidogenesis by prionoid-functionalized AuNRs. Pre-amyloidogenic RepA-WH1 monomers (stars) are generated on the AuNR surface from the initial RepA-WH1 dimers (cubes).[15a] Such functionalization induces the formation of oligomers that can be used as seeds for amyloid fibrillation.

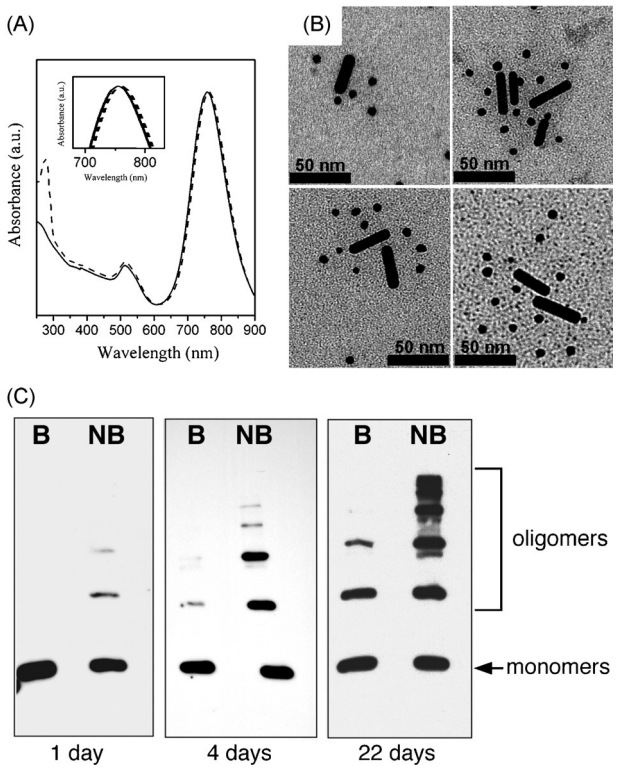

Figure 1. A) UV/Vis spectra of AuNRs in the absence (solid line) and presence (dash line) of H6-RepA-WH1(A31V) after 24 h of incubation (1:10^5 AuNR:H6-RepA-WH1(A31V) molar ratio with 20 μM of protein). The inset shows a detail of the 5 nm red shift observed under incubation. B) iEM of AuNRs incubated with H6-RepA-WH1(A31V) in (A) and the primary antibody (*anti*-WH1), attached to secondary Au-conjugated antibody clusters. C) SDS-PAGE plus western-blotting (*anti*-WH1) of the AuNRs in (B). B tracks: boiled samples; NB tracks: not boiled. The protein undergoes oligomerization on the particles, indicating the transition to a pre-amyloidogenic state.

AuNRs were first functionalized with thiolated polyethylene glycol to provide colloidal stability in buffer media and co-functionalized with lipoic acid (see the Supporting Information).[17] Immobilization of H6-RepA-WH1(A31V) was achieved after the specific modification of the AuNR surface with the lipoic amide-nitrilotriacetic-Co^{II} complex (ANTACo).[18] This chemical functionality specifically reacts with the H6 hexa-histidine chain (Scheme 1), avoiding undesired coupling to any of the multiple free amine groups in the protein. The ANTACo-functionalized AuNRs were incubated at 1:10^5 and 1:50 AuNR:H6-RepA-WH1(A31V) molar ratios, with protein concentrations of 20 and 0.1 μM, respectively. This protein forms a stable dimer in solution under a broad range of conditions (Scheme 1).[13a,14,19] However, the observed 5 nm red shift of the AuNRs' longitudinal localized surface plasmon resonance (LSPR) at both molar ratios, indicates the absence of AuNR self-assembly in solution (Figure 1 A, see the Supporting Information).[20] This might be expected from the presence of two oppositely anchored H6 groups on the H6-RepA-WH1(A31V) dimers (Scheme 1). These results point to the immobilization of the protein in its pre-amyloidogenic monomeric state on the metal surface, which is a necessary intermediate step in the ligand-promoted assembly of the protein as amyloids.[13a,14,19] The same incubation experiments were performed with spherical AuNPs of comparable (ca. 2×10^3 nm^2) and larger (ca. 1.1×10^4 nm^2) surface areas. Non-significant changes of the LSPRs were observed (see the Supporting Information), showing the convenience of using AuNRs for monitoring the protein functionalization process.

After 24 h, the mixture at the 1:10^5 AuNR:H6-RepA-WH1(A31V) molar ratio was centrifuged to separate the precipitate formed during the incubation, containing AuNRs and protein aggregates, from the soluble H6-RepA-WH1-(A31V). No precipitation of the protein was observed under the same conditions in the absence of AuNRs. Finally, the pellet was redispersed in buffer. To verify the coating of AuNRs by H6-RepA-WH1(A31V), immunoelectron microscopy (iEM) was carried out using a polyclonal *anti*-WH1 antibody (see the Supporting Information).[13c] Secondary antibodies conjugated to the spherical AuNPs (10 nm Ø) were consistently found around the AuNRs (7:1), although some unattached protein aggregated in the background (1:1) (Figure 1 B, see the Supporting Information). When the mixture

was stored for long periods of time (up to 4 weeks) at 4 °C, several oligomeric species of H6-RepA-WH1(A31V) were identified by means of denaturing gel electrophoresis (SDS-PAGE). The presence of a ladder with progressively higher molecular weights (Figure 1 C) reveals protein complexes that persisted under the extreme denaturing conditions (detergent plus boiling) of the electrophoresis (see the Supporting Information), consistent with the high stability of amyloids.[15b] This result suggests a dynamic process in which, over time, amorphous pre-amyloidogenic aggregates are converted into amyloid oligomers.

Immunoblotting with B3h7, an antibody specific for an oligomeric and pre-amyloidogenic form of H6-RepA-WH1-(A31V),[13c] yielded more intense binding to a protein sample stored for 22 days than to the native protein, even at the highest dilution of the antigen (Figure 2 A, see the Supporting Information). However, the conformation-unspecific *anti*-WH1 antibody recognized both samples equally well at their full range of concentrations. This experiment clearly demonstrates that the oligomers nucleated by AuNRs are amyloidogenic in nature. When such oligomers were used as seeds (that is, polymerization-nucleating agents) in incubations with soluble and untagged RepA-WH1(A31V), characteristic amyloid straight and unbranched fibers with 24.6 ± 0.7 nm cross-sectional thickness were grown, as observed by TEM analysis (Figure 2 B).[13a,14] Analogous experiments showed that occasional and less-structured fibers were formed in the presence of non-functionalized AuNRs (see the Supporting Information), which highlight the importance of the prionoid functionalization in the fibrillation.

Additionally, we used SERS spectroscopy to explore the transition from α-helix to β-sheet conformation (a signature for amyloidogenesis) in the oligomers obtained after the incubation of H6-RepA-WH1(A31V) with AuNRs. The SERS spectra of the native proteins and their oligomers were obtained using citrate-coated AuNPs (60 nm Ø) (Figure 3 A, see the Supporting Information), because of their high performance and plasmonic efficiency in SERS when aggregated on a substrate.[21] SERS spectra were collected using 785 nm laser light as the excitation source, at low intensity (1.4 $\mu W\,cm^{-2}$) to avoid damaging the samples. Under such conditions, the typical band broadening characteristic of the Raman spectra of proteins was observed.[22] SERS spectra were obtained for the native protein and at the initial (1 day) and final (22 days) stages of oligomerization. Incubation of H6-RepA-WH1(A31V) with AuNRs induced variations in

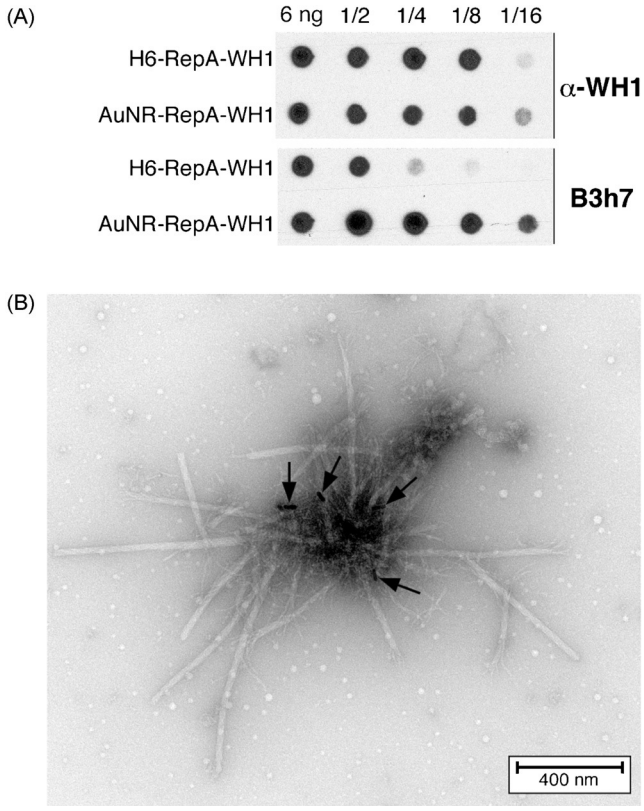

Figure 2. A) The dot-blot assay with B3h7, an antibody specific for amyloidogenic RepA-WH1 oligomers,[13c] reveals that the H6-RepA-WH1(A31V) protein assemblies around the AuNRs (even rows) are amyloids, whereas the soluble protein molecules (odd rows) are not. B) Mature AuNRs incubated with H6-RepA-WH1(A31V) (indicated by arrows) nucleate the growth of RepA-WH1(A31V) amyloid fibers.

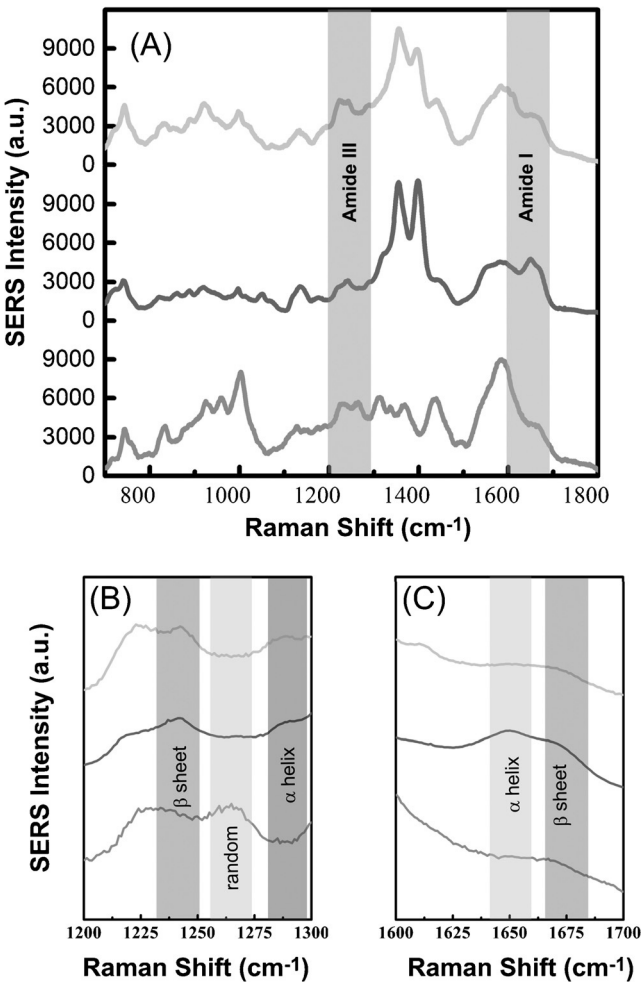

Figure 3. A) SERS spectra of the native protein dimers (bottom) and amyloid oligomers of low (middle) and high molecular weights (top), excited at 785 nm. B,C) Magnification of the amide III and I regions, respectively.

the full range of the SERS spectrum, as compared to the native protein (Figure 3, see Table 1 in the Supporting Information). Non-significant changes in the positions of the Raman signals were observed at different stages of the oligomerization, but line broadening resulted as the molecular weight of the oligomers increased.

Information about modifications in the tertiary structure of the oligomers can be extracted from changes at the low wavenumber region of the SERS spectra. This is the case for the two new intense bands at 1357 and 1399 cm^{-1}, associated with the C–C stretching, C–H deformation, and backbone vibrations (Figure 3 A). Although it is not possible to directly relate these bands to the amyloid conformation, their presence in the oligomers, but not in the native protein, clearly indicates a rearrangement in H6-RepA-WH1(A31V) when amyloidogenesis occurs.

Regarding the amyloid structure, the interactions between the backbone amide and carbonyl groups through hydrogen bonding, such as those responsible for the β-sheet structure in the amyloid fold, present nine vibrational modes, of which amides III and I are highly sensitive to changes in the secondary structure. The former ranges from 1220 and 1300 cm^{-1} (Figure 3 B), while the latter occurs between 1600 and 1700 cm^{-1} (Figure 3 C).[5,17] The amide III region of the native conformation is dominated by bands at 1222 and 1265 cm^{-1}, which are linked to aromatic residues and a random structure, whereas amide I does not show any Raman signal. On the other hand, we can observe two new bands at 1242 and 1290 cm^{-1}, attributed to the formation of β-sheets and the deformation of α-helices, respectively.[22] The latter might reflect the formation of a β-solenoid, a helical arrangement of β-strands common to some amyloid proteins.[23] This observation is also supported by two new bands at 1648 and 1670 cm^{-1} in the amide I region, which correspond to the α-helix and β-sheet secondary structures, respectively.

In summary, we have provided evidence for the feasibility of using prionoid-functionalized AuNRs as nucleating agents for controlled protein amyloidosis in vitro. The proposed mechanism of AuNR-mediated amyloid nucleation is based on a conformational change from the dimer protein precursor to the immobilized pre-amyloidogenic monomer at the nanoparticle surface, which promotes efficient amyloid oligomerization and fibrillation. Our results show the potential of using prionoid-functionalized AuNRs to understand amyloid oligomer formation and the disadvantage of such strategy to achieve early detection of amyloid diseases in vitro and in vivo, considering that the presence of the AuNPs can itself be amyloidogenic. We are currently exploring the possibility of using this system as a controlled model to understand protein amyloidogenesis in vivo.

Acknowledgements

Research at the R.G. laboratory was supported by MINECO grants CSD2009-00088, BIO2012-30852 and BIO2015-68730-R. Research at the A.G-M. and L.M.L-M. laboratories was supported by MINECO (MAT2014-59678-R and MAT2013-46101-R), Madrid Regional Government (S2013/MIT-2807) and the "I Convocatoria de Ayudas Fundación BBVA a Investigadores, Innovadores *y* Creadores Culturales" (14_CBB_147) grants. A.G-M. and G.G-R. acknowledge, respectively, receipt of Ramón *y* Cajal and FPI Fellowships from the Spanish MINECO.

Keywords: amyloidosis · gold nanorods · oligomers · prions · SERS

How to cite: *Angew. Chem. Int. Ed.* **2016**, *55*, 11237–11241
Angew. Chem. **2016**, *128*, 11403–11407

[1] P. Westermark, M. D. Benson, J. N. Buxbaum, A. S. Cohen, B. Frangione, S. Ikeda, C. K. Masters, G. Merlini, M. J. Saraiva, J. D. Sipe, *Amyloid* **2002**, *9*, 197–200.
[2] T. P. J. Knowles, M. Vendruscolo, C. M. Dobson, *Nat. Rev. Mol. Cell Biol.* **2014**, *15*, 384–396.
[3] a) T. Eichner, S. E. Radford, *Mol. Cell* **2011**, *43*, 8–18; b) A. K. Schütz, A. Soragni, S. Hornemann, A. Aguzzi, M. Ernst, A. Böckmann, B. H. Meier, *Angew. Chem. Int. Ed.* **2011**, *50*, 5956–5960; *Angew. Chem.* **2011**, *123*, 6078–6082.
[4] C. Wu, Z. Wang, H. Lei, Y. Duan, M. T. Bowers, J. E. Shea, *J. Mol. Biol.* **2008**, *384*, 718–729.
[5] a) N. P. R. Nilsson, *FEBS Lett.* **2009**, *583*, 2593–2599; b) R. Giraldo, J. M. Andreu, R. Díaz-Orejas, *EMBO J.* **1998**, *17*, 4511–4526.
[6] a) I. Choi, Y. S. Huh, D. Erickson, *Microfluid. Nanofluid.* **2012**, *12*, 663–669; b) R. A. Álvarez-Puebla, A. Agarwal, P. Manna, B. P. Khanal, P. Aldeanueva-Potel, E. Carbó-Argibay, N. Pazos-Pérez, L. Vigderman, E. R. Zubarev, N. A. Kotov, L. M. Liz-Marzán, *Proc. Natl. Acad. Sci. USA* **2011**, *108*, 8157–8161; c) L. Guerrini, R. Arenal, M. Benedetta, F. Chiti, R. Pini, P. Matteini, R. A. Alvarez-Puebla, *ACS Appl. Mater. Interfaces* **2015**, *7*, 9420–9428; d) I.-H. Chou, M. Benford, H. T. Beier, G. L. Coté, *Nano Lett.* **2008**, *8*, 1729–1735.
[7] G. J. Takashi, T. J. Miura in *Proteins: Structure, Function, and Engineering* (Ed.: B. B. Biswas, S. Roy), Springer Science, New York, **1995**, pp. 55–99.
[8] a) C. Cabaleiro-Lago, F. Quinlan-Pluck, I. Lynch, K. A. Dawson, S. Linse, *ACS Chem. Neurosci.* **2010**, *1*, 279–287; b) A.-M. Yousefi, Y. Zhoy, A. Querejeta-Fernández, K. Sun, N. A. Kotov, *J. Phys. Chem. Lett.* **2012**, *3*, 3249–3256; c) Z. S. Al-Garawi, J. R. Thorpe, L. C. Serpell, *Angew. Chem. Int. Ed.* **2015**, *54*, 13327–13331; *Angew. Chem.* **2015**, *127*, 13525–13529.
[9] Y.-H. Liao, Y.-J. Chang, Y. Yoshiike, Y.-C. Chang, Y.-R. Chen, *Small* **2012**, *8*, 3631–3639.
[10] D. A. Yanina, J. A. Fauerbach, J. V. Pellegrotti, T. M. Jovin, E. A. Jares-Erijman, F. D. Stefani, *Nano Lett.* **2013**, *13*, 6156–6163.
[11] Y. Kim, J.-H. Part, H. Lee, J.-M. Nam, *Sci. Rep.* **2016**, *6*, 19548.
[12] J. L. Silva, L. M. Lima, D. Foguel, Y. Cordeiro, *Trends Biochem. Sci.* **2008**, *33*, 132–140.
[13] a) R. Giraldo, *Proc. Natl. Acad. Sci. USA* **2007**, *104*, 17388–17393; b) F. Gasset-Rosa, M. J. Maté, C. Dávila-Fajardo, J. Bravo, R. Giraldo, *Nucleic Acids Res.* **2008**, *36*, 2249–2256; c) M. Moreno-del Álamo, S. Moreno-Díaz de la Espina, M. E. Fernández-Tresguerres, R. Giraldo, *Sci. Rep.* **2015**, *5*, 14669–14672; d) C. Fernández, R. Nuñez-Ramírez, M. Jiménez, G. Rivas, R. Giraldo, *Sci. Rep.* **2016**, *6*, 23144.
[14] E. Torreira, M. Moreno-del Álamo, M. E. Fuentes-Perez, C. Fernández, J. Martín-Benito, F. Moreno-Herrero, R. Giraldo, O. Llorca, *Structure* **2015**, *23*, 183–189.
[15] a) M. E. Fernández-Tresguerres, S. Moreno-Díaz de la Espina, F. Gasset-Rosa, R. Giraldo, *Mol. Microbiol.* **2010**, *77*, 1456–1469; b) F. Gasset-Rosa, A. S. Coquel, M. Moreno-del Álamo,

P. Chen, X. Song, A. M. Serrano, M. E. Fernández-Tresguerres, S. Moreno-Díaz de la Espina, A. B. Lindner, R. Giraldo, *Mol. Microbiol.* **2014**, *91*, 1070 – 1087.
[16] C. J. Murphy, T. K. Sau, A. M. Gole, C. J. Orendorff, J. Gao, L. Gou, S. E. Hunyadi, T. Li, *J. Phys. Chem. B* **2005**, *109*, 13857 – 13870.
[17] E. Oh, K. Susumu, A. J. Mäkinen, J. R. Deschamps, A. L. Huston, I. L. Medintz, *J. Phys. Chem. C* **2013**, *117*, 18947 – 18956.
[18] J. M. Abad, S. F. L. Mertens, M. Pita, V. M. Fernández, D. J. Schiffrin, *J. Am. Chem. Soc.* **2005**, *127*, 5689 – 5694.
[19] R. Giraldo, C. Fernández-Tornero, P. R. Evans, R. Díaz-Orejas, A. Romero, *Nat. Struct. Biol.* **2003**, *10*, 565 – 571.
[20] a) A. Guerrero-Martínez, M. Grzelczak, L. M. Liz-Marzán, *ACS Nano* **2012**, *6*, 3655 – 3662; b) K. K. Caswell, J. N. Wilson, U. H. F. Bunz, C. J. Murphy, *J. Am. Chem. Soc.* **2003**, *125*, 13914 – 13915.
[21] a) C. Costas, V. López-Puente, G. Bodelón, C. González-Bello, J. Pérez-Juste, I. Pastoriza-Santos, L. M. Liz-Marzán, *ACS Nano* **2015**, *9*, 5567 – 5576; b) C. Hamon, M. S. Novikov, L. Scarabelli, D. M. Solís, T. Altantzis, S. Bals, J. M. Taboada, F. Obelleiro, L. Liz-Marzán, M. Luis, *ACS Photonics* **2015**, *2*, 1482 – 1488.
[22] D. Nemecek, J. Stepankek, G. J. Thomas, *Current Protocols in Protein Science.* **2013**, 71, 17.8:17.8.1 – 17.8.52.
[23] A. V. Kajava, U. Baxa, A. C. Steven, *FASEB J.* **2010**, *24*, 1311 – 1319.

Received: May 20, 2016
Revised: June 30, 2016
Published online: August 4, 2016

